

Evaluation of the Power Generation Efficiency and the Amount of CO₂ Discharge from a Microgrid Using a Fuel Cell Cascade System

Shin'ya Obara*

*Power Engineering Laboratory, Department of Electrical and Electronic Engineering, Kitami

Institute of Technology

165 Koen-cho, Kitami, Hokkaido 090-8507, Japan

E-mail: obara@mail.kitami-it.ac.jp

Phone/FAX +81-157-26-9262

Abstract

The purpose of this study was to combine fuel cells with different operating temperatures into fuel cell cascade systems in order to analyze their power generation efficiency and environmental impact (CO₂ emissions). Nine fuel cell cascade systems were investigated by numerical analysis. We also proposed the use of these systems in microgrids. The power generation efficiency of a compound system containing a solid-oxide fuel cell, a micro-gas turbine, a reformer, and a proton-exchange membrane fuel cell showed great improvement compared with simplex operation of each component of the system. Moreover, a fuel cell cascade system can use alcohol fuels with low CO₂ emission factors without reducing the power generation efficiency. The fuel cell cascade systems tested showed that CO₂ emission reductions are possible.

Keywords: Fuel cell, Cascade system, Compound system, PEFC, SOFC, Micro-gas turbine, Microgrid.

1. Introduction

Small-scale microgrids are growing in popularity as development of a future distributed power supply continues [1, 2]. Consequently, analysis is needed for power generation systems servicing small-scale microgrids composed of 10 to 100 houses. The average power supply of a microgrid of this size is typically below 100 kW. Fuel cells such as solid-oxide fuel cells (SOFCs) and proton-exchange membrane fuel cells (PEFCs), as well as heat engines such as the micro-gas turbine (MGT) and the gas engine, can be used for power generation for microgrids requiring less than 100 kW. These generators have optimum operating temperatures, and the power output characteristics can differ as a result of the environmental characteristics. To make effective use of the fuel supplied to a system, it is best to use the generating equipment at suitable operating temperatures; the temperature range can vary from ambient temperature to high temperatures. Moreover, if the system's characteristic load factors, power generation efficiency, and CO₂ emissions are taken into consideration during optimum operation planning, a high-efficiency system with a low environmental impact can be built. A generator designed for the appropriate operating temperature can be introduced into each temperature span from high temperature to low temperature. This compound energy system is described as a cascade system. A compound power system containing two or more types of fuel cells and the combined power system of a fuel cell and a heat engine are also described as fuel cell cascade systems.

The aim of this study is to clarify the composition and operation method of a system with high power generation efficiency and low environmental impact: i.e., introducing a fuel cell cascade system into a small-scale microgrid. This paper examines a cascade system composed of an SOFC [3, 4], a PEFC [5, 6], an MGT, and methanol steam reforming equipment [7, 8] through a numerical analysis. The performance of a compound system composed of an SOFC and an MGT has been investigated previously through experiments and analysis [9, 10]. However, there are no published studies evaluating the power generation characteristics and the environmental-impact characteristics of introducing these systems into the load pattern of a small-scale microgrid. Moreover, though the operation of a compound SOFC and PEFC system has also been investigated [11], a compound installation containing an MGT and an SOFC-PEFC combined system has not been previously described. Finally, there are currently no studies investigating the system performance when a fuel cell cascade system is introduced into a microgrid. Therefore, in this paper, the power generation efficiency and environmental impact of fuel cell cascade systems containing two or more individual fuel cells are compared, and a high-performance power source for microgrids is proposed.

2. Compound Energy System

2.1 Microgrid using fuel cell cascade system

Today, in large-scale electric power systems in urban areas, electric power is supplied from several mixed power generation methods. The planning and operation of the system take into

consideration the characteristics of each power generation method. Figure 1 shows the relationship between capacity and efficiency in power generation technology. The capacities of most electric power systems in urban Japan are not less than 1000 kW. Examples of generation technology include steam turbines, gas turbines, gas engines, SOFCs, and MCFCs (molten carbonate fuel cells). The power generation efficiency of a compound system containing an SOFC, an MCFC, and an SOFC and an MCFC is high compared with an engine generator. The electric power supplied by a microgrid can be drawn from systems with various power generation capacities. In this paper, an independent power-source system introduced into the microgrid for 10 to 100 houses is investigated. From Fig. 1, it can be seen that an SOFC, a PEFC, a gas engine, and an MGT would be effective in this case.

2.2 Compound power generation system

2.2.1 Scope of investigation

In order to use the energy of fossil fuel effectively, the energy system is introduced in stages for each temperature span from high temperature to low temperature (outside air temperature). Figure 2 shows an example of a power generation cascade system. The combination system shown in Fig. 2, which is applicable to a microgrid for 10 to 100 houses, is restrained from the power generation capacity expressed in Fig. 1. In this paper, nine systems (EQ 1 to EQ 9, shown in Table 1) are investigated. Both EQ 1 and EQ 2 are independent PEFC systems; EQ 1 uses steam reforming of methanol (bio-methanol), and EQ 2 uses steam reforming of natural gas. EQ 3 and EQ 4 are

independent SOFC and MGT systems with fuel supplies of natural gas. EQ 5 and EQ 6 are compound systems containing an SOFC and a PEFC. Reformed gas obtained from methanol steam reforming that utilizes the exhaust heat of the SOFC is used for fuel for the PEFC. EQ 7 is a compound SOFC and MGT system utilizing natural gas. EQ 8 and EQ 9 are compound systems that combine an SOFC, an MGT and a PEFC. The reformed gas obtained by methanol steam reforming from the exhaust heat of the SOFC is used for fuel in the PEFC of EQ 8 and EQ 9, just as in EQ 5 and EQ 6. The operation method of the methanol-reforming equipment differs between EQ 5 and EQ 6 and between EQ 8 and EQ 9. On the other hand, the operation method of the methanol-reforming equipment is the same in EQ 5 and EQ 8 and in EQ 6 and EQ 9. The difference in the operation of the methanol-reforming equipment is described in Sections 2.3 and 3.1.

2.2.2 Equipment capacity introduced into compound energy system

The power generation capacity of the component of each system is described in Table 1. Although more detail is given in Section 3.3, the power load of a microgrid was assumed to be 30 kW maximum. Therefore, the power generation capacity of an independent system (from EQ 1 to EQ 4) was established as 30 kW. The decision process of determining the power generation capacity of each component (the SOFC and the PEFC of the SOFC-PEFC compound system [EQ 5, EQ 6]) is described in Section 3.1 (3); we will first determine the capacity of EQ 6. The capacity of each component in EQ 5 was established in a manner similar to the method used for EQ 6. The power generation capacity of the components of EQ 7, in which the MGT is operated with the exhaust heat

of the SOFC, was taken from a reference [9]. For EQ 8, if the reference value is used to determine the power generation capacity of one of the components, the value will become so small that the capacity of the MGT is difficult to realize. Consequently, all capacities for the SOFC, the PEFC, and the MGT were set to 10 kW. Moreover, although the power generation capacity of each piece of equipment in EQ 9 is set, the amount of exhaust heat from the SOFC-MGT compound system was first calculated based on reference [9]. The capacity of the PEFC was determined by the same method described in Section 3.1 (3).

2.3 Operating temperature of the generating equipment

Figure 3 shows the relationship between the operating temperature and the exhaust heat temperature for each system from EQ 1 to EQ 9. The number described into () in this figure is the temperature used in the analysis presented in this paper. For example, although the operating temperature of the SOFC is 700 °C to 1000 °C, 1000 °C was used in the analysis. Moreover, the exhaust heat temperature of the SOFC is 600 °C to 900 °C, and the operating temperature used in the analysis of the MGT was 900 °C.

2.4 Production of reformed gas and supply method to the PEFC

The PEFC contained in EQ 5, EQ 6, EQ 8 and EQ 9 uses the reformed gas obtained by methanol steam reforming. The production methods for the reformed gas and the supply methods to the PEFC are described in the following section.

2.4.1 Compound system without storage of reformed gas

When the power load of a microgrid exceeds the capacity of the SOFC, reformed gas is produced from methanol by supplying the exhaust heat of the SOFC to the reformer in EQ 5. The power demand of the microgrid is met by supplying this reformed gas to the PEFC. However, when the exhaust heat of the SOFC cannot fill the demand, the combustion heat of natural gas is supplied to the reformer. EQ 8 and EQ 5 produce reformed gas from methanol by supplying the exhaust heat of the SOFC and the MGT to a reformer when the power load of the microgrid exceeds the capacity of the SOFC-MGT compound system. On the other hand, when the exhaust heat from the SOFC and the MGT is insufficient to supply the reformed gas demanded by the PEFC, additional heat is supplied to the reformer from the combustion heat of natural gas.

2.4.2 Compound system with storage of reformed gas

Reformed gas is always produced by the steam reforming of methanol using the exhaust heat of the SOFC or the SOFC-MGT compound systems in EQ 6 and EQ 9. The reformed gas produced is compressed by a compressor and stored in a cylinder. If the power load demand of the microgrid exceeds the capacity of the SOFC or the SOFC-MGT compound system, in order to avoid a power failure, stored reformed gas will be supplied to the PEFC. Although EQ 6 and EQ 9 require a compressor and a cylinder, the capacity of a reformer is still small compared with EQ 5 and EQ 8. Moreover, the exhaust heat of the system can be stored as reformed gas.

3. Operation Method of the Fuel Cell Cascade System

3.1 Composition of a cascade system

The nine systems shown in Table 1 are operated by the following five methods. The power generation efficiency and the CO₂ emissions of each operation method were investigated by numerical analysis.

(1) Single type

As shown in Fig. 4 (a), in this setup, electric power is supplied to a microgrid from one kind of generating equipment. This operation method has lots of operating time involving partial-load operation with low efficiency. If a load factor (production of electricity / power generation capacity x 100 [%]) is less than 30%, operation of the SOFC and the SOFC-MGT compound system becomes difficult. Because partial loads occur frequently in the operation of a microgrid for houses, it is expected that the power generation efficiency of this operation method will be low. Figure 4 (a) and Table 1 show the operating method for EQ 1, EQ 2, EQ 3 and EQ 4.

(2) Two types of equipment combined in a cascade system

Because the operation method using a single type of equipment cannot generate high power efficiency, Fig. 4 (b) considers the sharing of a load between two kinds of generating equipment. The pieces of generating equipment differ in their partial-load performance. Consequently, Equipment A,

which has a high maximum power generation efficiency, is made to correspond to a fixed base load, while Equipment B, which has a high power generation efficiency under a partial load, is made to correspond to a fluctuating load.

The operating method of EQ 5 and EQ 7 is shown in Fig. 4 (b). Reformed gas from methanol is supplied to the PEFC of EQ 5 as a fuel. This reformed gas is produced by supplying the SOFC exhaust heat to a reformer whenever the power load of the microgrid exceeds the base load of Equipment A (SOFC). The combustion gas is supplied to the reformer by burning natural gas separately to produce the amount of reformed gas required for the PEFC when the SOFC exhaust heat is insufficient.

(3) Two types of equipment combined in a cascade system with time-shift utilization of reformed gas

Figure 4 (c) shows the operating method for EQ 6. As mentioned in Section 2.4.2, reformed gas is always produced by methanol steam reforming using the exhaust heat from the SOFC in EQ 6. After removing the water and the CO in the reformed gas, the reformed gas is compressed and stored in a cylinder. The capacity of the SOFC determines the amount of reformed gas produced by the exhaust heat of the SOFC, based on load balancing estimation and the amount of demanded reformed gas [11]. If the power load exceeds the base load of Equipment A (SOFC), as shown in Fig. 4 (c), the reformed gas from the cylinder will be supplied to Equipment B (PEFC).

(4) Three types of equipment combined in a cascade system

Figure 4 (d) shows the operation method of EQ 8: load sharing by three kinds of generating equipment. The three pieces of generating equipment correspond to a base load, a middle load, and a peak load: the SOFC with the highest maximum power generation efficiency is used to meet the base load demand (Equipment A), the MGT utilizing the high-temperature exhaust heat from the SOFC is used to meet the middle load demand (Equipment B), and the PEFC with methanol steam reforming that performs well under a partial load is used to meet the peak load demand (Equipment C).

The reformed gas supplied to the PEFC is produced using the exhaust heat (SOFC and MGT) of the system. The reformed gas is produced, as in EQ 5, in the period when the power load exceeds the base load and the middle load supplied by Equipment A (SOFC) and Equipment B (MGT). Moreover, when the amount of exhaust heat from the SOFC and the MGT are not sufficient to supply the amount of reformed gas required by the PEFC, the system supplies natural gas separately.

(5) Three types of equipment in a combined cascade system with time shift utilization of reformed gas

Although the composition of the system is the same as (4), the throughput time of the reformed gas and the supplying time to the PEFC are the same as in (3) (Figure 4 [c]).

3.2 Performance of generating equipment

Figure 5 shows the relation of the load factor and the power generation efficiency of an MGT, an SOFC, a PEFC, and an SOFC-MGT compound system [9, 12-14]. The power generation efficiency of an SOFC (Fig. 5 [b]) and an SOFC-MGT compound system (Fig. 5 [e]) is higher than that of other generating equipment. However, the power generation efficiency at partial loads is low for these types of equipment. If the load factor is less than 40%, the power generation efficiency will fall greatly, and stable operation becomes difficult if the load factor is less than 30%. The power generation efficiency with and without the methanol reformer are shown in the performance of the PEFC in Fig. 5 (d). Although the reforming component efficiency $\eta_{r,t}$ was defined by Eq. (1), it was set to a constant 75% in this paper, regardless of the load factor under investigation.

$$\eta_{r,t} = \frac{\text{The calorific power of hydrogen in reformed gas}}{\text{The heating value of the heat source of a reformer} + \text{The calorific power of reforming fuel}} \cdot 100[\%] \quad (1)$$

3.3 Power load pattern

Three power demand patterns are shown in Fig. 6.

The average load pattern is the power load of a microgrid on representative days in February in 30 houses in Sapporo, Japan [15]. Air conditioning is not used for the summer season (from July to September) in the average house in Sapporo. Moreover, because the space-heating load of winter (from November to March) uses the exhaust heat of the power generation system, it is not contained in the power load shown in Fig. 6. Therefore, because the power load pattern shown in Fig. 6 is the

load of electric lights and home electric appliances, the difference in the average load is very small between months.

Two additional patterns created from the average load pattern shown in Fig. 6 were also investigated. The compressed load pattern in Fig. 6 makes the width of the fluctuating load smaller than the average load pattern. In contrast, the extended load pattern makes the width of the fluctuating load larger than the average load pattern. These two patterns represent 50% compression and 150% expansion beyond the average power demand load of a representative day. The integrated value (power demanded on a given day) of the load of each pattern is the same as the integrated average load pattern.

4. Analysis Results

4.1 Power generation efficiency and CO₂ discharge characteristics

Figure 7 shows the analysis results for the power generation efficiency (Fig. 7 [a]) and the CO₂ emissions (Fig. 7 [b]) of the nine power generation systems (EQ1 to EQ9). The average load pattern shown in Fig. 6 was used for the power load pattern of the microgrid. The CO₂ emissions were calculated from the type of fuel and the consumption of the system. In this case, the CO₂ emission factor [16] was used.

The power generation efficiencies of EQ 1, EQ 2, and EQ 4 were low, and the power generation efficiencies of EQ 7, EQ 8, and EQ 9 were high, as seen in Fig. 7 (a). EQ 1, EQ 2, and EQ 4 are the single-equipment setups shown in Fig. 4 (a). EQ 7, EQ 8, and EQ 9 are the operation methods shown

in Figs. 4 (b), (d), and (e), respectively. EQ 8 had the best power generation efficiency at almost all times. This demonstrates that the method of using an SOFC, an MGT, and a PEFC as a cascade system, as shown in Figs. 2 and 3, is effective. The power generation efficiency of EQ 9 was low compared with EQ 8, showing that the method of always producing reformed gas by steam reforming of methanol using the exhaust heat of a system and supplying this storage gas to the PEFC with a time shift actually reduces the power generation efficiency.

From the results shown in Fig. 7 (b), it can be seen that EQ 4 and EQ 1 had high CO₂ emissions. In the time from 17:00 to 21:00, EQ 8 had high CO₂ emissions. This occurred because the amount of exhaust heat produced by the SOFC-MGT compound system could not provide the quantity of methanol reforming gas that the PEFC required. As a result, it was necessary to supply natural gas to the reformer so that the required amount of reformed gas could be provided. Therefore, compared with the EQ 9 system, which always produces reformed gas from methanol fuel using exhaust heat and has a small CO₂ emission factor, EQ 8 had high CO₂ emissions. Because the combination of the capacity of each piece of equipment (SOFC, MGT, PEFC) from EQ 8 and EQ 9 differs and because the load factor changes with differences in load, the results of the power generation efficiency and CO₂ emissions of the systems differ.

Because the only fuel used in EQ 2 was methanol, there were very few CO₂ emissions compared with other systems using natural gas.

4.2 Influence of load patterns

Figures 8 (a) to (f) show the analysis results for the power generation efficiency and the CO₂ emissions for each system under the three load patterns shown in Fig. 6.

(1) PEFC (EQ 1, EQ 2)

From Fig. 8 (a), the efficiency at the time that EQ 1 and EQ 2 were operating under the extended load pattern was reduced in the period from 0:00 to 5:00 for a small load. The CO₂ emissions from EQ 2, which used methanol fuel, were greatly reduced compared with EQ 1, which used natural gas.

(2) SOFC (EQ 3)

Figure 8 (b) shows the SOFC individual operations. The power generation efficiency under the compressed load pattern was 39% to 50% of the high value. However, the power generation efficiency under average load patterns and extended load patterns was greatly reduced compared with the PEFC (Fig. 8 [a], EQ 1 and EQ 2) from 0:00 to 5:00 with a small load. If the SOFC is introduced into a large load fluctuation pattern, the power generation efficiency will decrease greatly at the time of the low load factor. The CO₂ emissions from this system (EQ 3) were much higher than those from EQ 2.

(3) MGT (EQ 4)

Figure 8 (c) shows the analysis results for the MGT.

The power generation efficiency of the MGT was low compared with the PEFC and the SOFC. Because natural gas consumption increases with low power generation efficiency, the CO₂ emissions of the MGT were high compared with those of the PEFC and the SOFC. However, because the MGT was not accompanied by fuel consumption when operating with the exhaust heat of the SOFC (EQ 7, EQ 8, EQ 9), there was no discharge of CO₂ from the MGT.

(4) SOFC-PEFC combined system (EQ 5, EQ 6)

Figure 8 (d) shows the analysis results for the power generation efficiency and the CO₂ emissions of an SOFC-PEFC compound system. The period from 0:00 to 5:00 had a low load, and the power generation efficiency during this period was slightly lower for EQ 6 than for EQ 5. However, the power generation efficiencies of EQ 5 and EQ 6 at other time periods were 40% to 50% of the high range. Because the PEFC was operated by a supply of methanol fuel, the CO₂ emissions of EQ 5 and EQ 6 were reduced compared with the SOFC individual system (Fig. 8 [b], EQ 3). Moreover, the CO₂ emissions for EQ 6 in which the reformed gas from methanol was always produced using the SOFC exhaust heat were lower than those for EQ 5. The amount of exhaust heat from the SOFC in EQ 5 could not provide the required amount of methanol reforming gas for the PEFC during the period from 17:00 to 21:00 when a large load was placed on the system. As a result, in order to supply the necessary reformed gas, natural gas was supplied to the reformer. Because of this, the CO₂ emissions for EQ 5 increased during this period.

(5) SOFC-MGT combined system (EQ 7)

Figure 8 (e) shows the analysis results for the power generation efficiency and the CO₂ emissions for the SOFC-MGT compound system. The system was influenced by the partial load performance of the SOFC, and the power generation efficiency during the time of low loading from 0:00 to 5:00 was greatly reduced. However, the power generation efficiency of EQ 7 during periods other than low loading was much greater than the SOFC-only system (Fig. 8 [b], EQ 3). This is because the MGT was operated by the SOFC exhaust heat and without a fuel supply. Because the power generation efficiency was good, the CO₂ emissions from EQ 7 were reduced compared with EQ 3.

(6) SOFC-MGT-PEFC combined system (EQ 8, EQ 9)

Figure 8 (f) shows the analysis results for the power generation efficiency and the CO₂ emissions for an SOFC-MGT-PEFC compound system. As Fig. 4 (d) shows, when the power load of the microgrid exceeded the capacity of Equipment A (SOFC) and Equipment B (MGT), reformed gas was produced using the exhaust heat of the SOFC and the MGT in EQ 8. Supplying this reformed gas to the PEFC corresponded to the fluctuating load. In contrast, EQ 9 always produced reformed gas by steam reforming of methanol using the exhaust heat of the SOFC and the MGT. The reformed gas produced was stored in a cylinder and supplied to the PEFC during the period from 17:00 to 21:00 when a large power load was present. EQ 9 generated electricity with the PEFC in the period with the large load using the reformed gas that had been stored up to that point. Therefore, EQ 9 experiencing a large load over a period of time did not increase the fuel supplied to

the SOFC. As a result, the power generation efficiency of EQ 9 from 17:00 to 21:00 increased greatly.

In contrast, the CO₂ emissions from EQ 8 showed the same tendency as EQ 5 (Fig. 8 [d]).

Accordingly, the amount of exhaust heat from the SOFC-MGT compound system did not provide the quantity of reformed gas that needed to be supplied to the PEFC for power generation during the large-load period. As a result, in order to supply the necessary reformed gas, additional natural gas was supplied to the reformer. Therefore, the CO₂ emissions from EQ8 increased during the time period with a large load.

4.3 Average power generation efficiency and the amount of CO₂ emissions

Figure 9 shows the average values for the power generation efficiency and the CO₂ emissions on a representative day. The systems with the highest power generation efficiencies were EQ 8, EQ 7, and EQ 9. The systems with the lowest CO₂ emissions were EQ 2, EQ 9, and EQ 7. The relation between each system and its power generation efficiency and CO₂ emissions (average value on a representative day) is shown in Fig. 10. The power generation efficiencies of the SOFC-MGT-PEFC compound system and the SOFC-MGT compound system were high. Therefore, as expected, the power generation efficiency of a fuel cell cascade system will also be high. Operation of a PEFC and an SOFC-MGT-PEFC compound system (the type that always produces reformed gas from the exhaust heat of the SOFC and the MGT) using methanol fuel produces few CO₂ emissions. Because fuel alcohols with low CO₂ emission factors can be used, CO₂ emissions can be reduced in a fuel cell cascade system.

5. Conclusions

Numerical analysis was used to estimate the power generation efficiency and the environmental impact (CO₂ emissions) of supplying electric power to a small-scale microgrid from a fuel cell cascade system. The following conclusions were obtained:

(1) If different types of fuel cells are used sequentially at given operating temperatures (cascade use), the power generation efficiency can be greatly improved compared with operation of a simple fuel cell. In the analysis presented in this paper, the power generation efficiencies of an SOFC-MGT-PEFC compound system (daily average power generation efficiency of 58.1% to 59.8%) and an SOFC-MGT compound system (daily average power generation efficiency of 51.0% to 55.6%) were high. The power generation efficiencies of fuel cell cascade systems are very good.

(2) There are few CO₂ emissions from a PEFC and an SOFC-MGT-PEFC compound system that is supplied with methanol fuel. The SOFC-MGT-PEFC compound system produces reformed gas from methanol steam reforming while using the exhaust heat of the SOFC and the MGT. After the system compresses this reformed gas, it stores it in a cylinder, and reformed gas is supplied to the PEFC during times of large loads. The fuel cell cascade system is capable of combining low-CO₂ emission fuel alcohol with a fossil fuel without an accompanying drop in power generation efficiency.

Acknowledgements

This study was supported by the Iwatani technology research grant. Gratitude is expressed to Iwatani Naoji Foundation.

References

- [1] D. V. Spitzley, G. A. Keoleian, S. G. Baron, Life cycle energy and environmental analysis of a microgrid power pavilion, *International Journal of Energy Research* 2007; **31(1)**, 1-13.
- [2] S. Vachirasricirikul, I. Ngamroo, S. Kaitwanidvilai, Application of electrolyzer system to enhance frequency stabilization effect of microturbine in a microgrid system, *International Journal of Hydrogen Energy* 2009; **34(17)** , 7131-7142.
- [3] M.M. Hussain, X. Li, I. Dincer, A numerical investigation of modeling an SOFC electrode as two finite layers, *International Journal of Hydrogen Energy* 2009; **34(7)** , 3134-3144.
- [4] I. Dincer, Environmental and sustainability aspects of hydrogen and fuel cell systems, *International Journal of Energy Research* 2007; **31(1)**, 29-55.
- [5] F. Urbani, O. Barbera, G. Giacoppo, G. Squadrito, E. Passalacqua, Effect of operative conditions on a PEFC stack performance, *International Journal of Hydrogen Energy* 2008; **33(12)** , 3137-3141.
- [6] M. Pehnt, Life-cycle assessment of fuel cell stacks, *International Journal of Hydrogen Energy* 2001; **26(1)** , 91-101.

- [7] B. Lindström, L. J. Pettersson, Hydrogen generation by steam reforming of methanol over copper-based catalysts for fuel cell applications, *International Journal of Hydrogen Energy* 2001; **26(9)** , 923-933.
- [8] F. Gallucci, A. Basile, S. Tosti, A. Iulianelli, E. Drioli, Methanol and ethanol steam reforming in membrane reactors: An experimental study, *International Journal of Hydrogen Energy* 2007; **32(9)** , 1201-1210.
- [9] P. Costamagna, L. Magistri, A. F. Massardo, Design and part-load performance of a hybrid system based on a solid oxide fuel cell reactor and a micro gas turbine, *Journal of Power Sources*; 2001, **96 (2)**, 352-368.
- [10] S. H. Chan, H. K. Ho, Y. Tian, Multi-level modeling of SOFC-gas turbine hybrid system, *International Journal of Hydrogen Energy* 2003; **28(8)** , 889-900.
- [11] S. Obara, Power generation efficiency of an SOFC-PEFC combined system with time shift utilization of SOFC exhaust heat, *International Journal of Hydrogen Energy* 2010; **35(2)** , 757-767.
- [12] K. Hori, Status of development of a polymer electrolyte fuel cell (PEFC), *Denki* 2004; **6**, 58-60. (in Japanese)
- [13] S. Obara and I. Tanno, Study on the polymer membrane-type fuel cell and hybrid hydrogenation engine system considering improvement of efficiency for partial-load operation, *Transactions of the ASME, Journal of Fuel Cell Science and Technology* 2008; **5(4)**, 1-10.
- [14] R. Bove, S. Ubertini, Modeling solid oxide fuel cell operation: Approaches, techniques and results, *Journal of Power Sources* 2006; **159 (1)**, 543-559.
- [15] K. Narita, *The Research on Unused Energy of the Cold Region City and Utilization for the District Heat and Cooling*, Ph. D. thesis, Hokkaido University, Sapporo, 1996.
- [16] Ministry of the Environment, *The Summary of the Calculation Method and Emission Factor in Calculation, Report and Official Announcement*, Government of Japan, 2010.

Captions

Table 1 Power generation equipment

Fig. 1 Power capacity and efficiency of the power system

Fig. 2 Cascade system introduced into a microgrid with 100 houses

Fig. 3 Fuel cell cascade system

Fig. 4 Operation methods of fuel cell cascades incorporated into a microgrid

(a) Single piece of equipment

(b) Two types of equipment in a combined cascade system

(c) Two types of equipment in a combined cascade system with time shift utilization of reformed gas

(d) Three types of equipment in a combined cascade system

(e) Three types of equipment in a combined cascade system with time shift utilization of reformed gas

Fig. 5 The relationship between the load factor and the power generation efficiency for each piece of equipment

(a) Micro-gas turbine (MGT)

(b) SOFC

(c) Natural-gas-supplied PEFC

(d) Methanol reformed gas-supplied PEFC

(e) SOFC and MGT combined system

Fig. 6 Power demand pattern of the microgrid (Sapporo, Japan, 30 houses, February representative day)

Fig. 7 Analysis results for the power generation efficiency and the CO₂ emissions for each piece of equipment under the average load pattern

(a) Average power generation efficiency

(b) CO₂ emissions

Fig. 8 Analysis results for the power generation efficiency and the CO₂ emissions of each piece of equipment under three load patterns

(a) PEFC (EQ 1, EQ 2)

(b) SOFC (EQ 3)

(c) MGT (EQ 4)

(d) SOFC-PEFC combined system (EQ 5, EQ 6)

(e) SOFC-MGT combined system (EQ 7)

(f) SOFC-MGT-PEFC combined system (EQ 8, EQ 9)

Fig. 9 Analysis results for the daily average power generation efficiency and the CO₂ emissions

(a) Power generation efficiency

(b) CO₂ emissions

Fig. 10 Analysis results for the daily average power generation efficiency and the CO₂ emissions

Table 1 Power generation equipment

EQ 1: Natural-gas supply PEFC (30 kW)
EQ 2: Methanol reformed gas supply PEFC (30 kW)
EQ 3: SOFC (30 kW)
EQ 4: Micro gas turbine (MGT) (30 kW)
EQ 5: SOFC-PEFC combined system (SOFC: 22 kW, PEFC: 8 kW)
EQ 6: SOFC-PEFC combined system with time shift of reformed gas (SOFC: 22 kW, PEFC: 8 kW)
EQ 7: SOFC-MGT combined system (SOFC: 25 kW, PEFC: 5 kW)
EQ 8: SOFC-MGT-PEFC combined system (SOFC: 10 kW, PEFC: 10 kW, MGT: 10 kW)
EQ 9: SOFC-MGT-PEFC combined system with time shift of reformed gas (SOFC: 19 kW, PEFC: 7 kW, MGT: 4 kW)

MCFC: Molten carbonate fuel cell, PEFC: Proton-exchange membrane fuel cell
SOFC: Solid-oxide fuel cell, MGT: Micro gas turbine

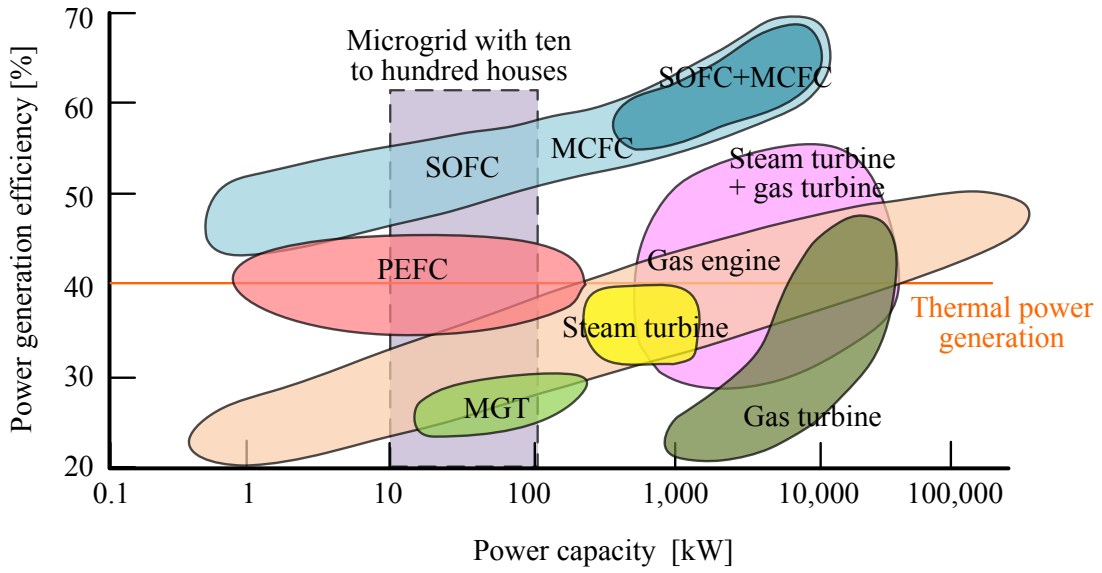


Fig. 1 Power capacity and efficiency of the power system

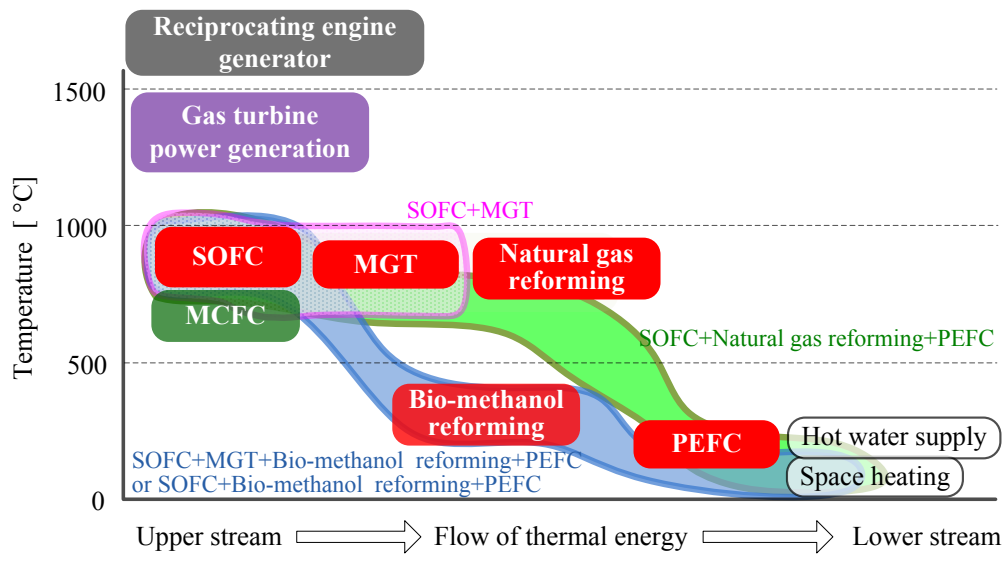


Fig. 2 Cascade system introduced into a microgrid with 100 houses

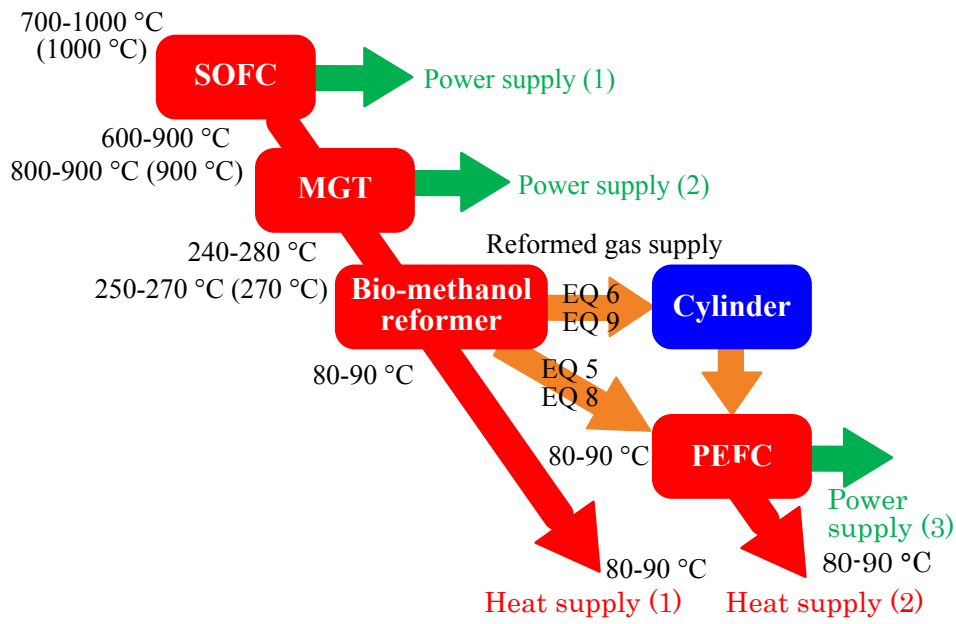
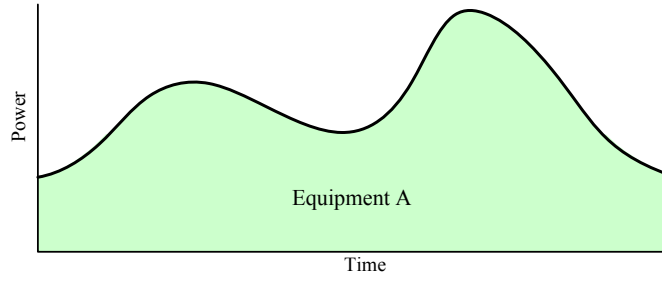
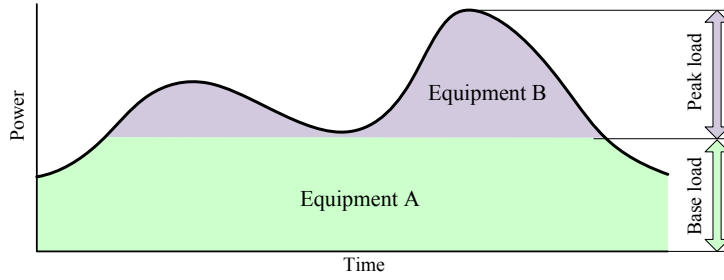


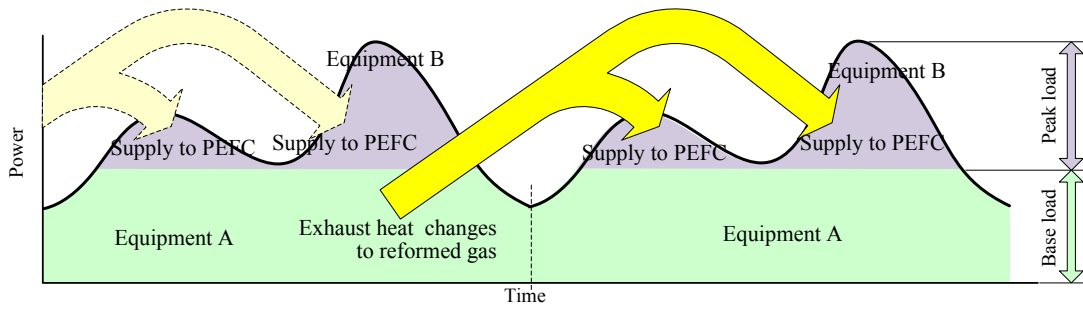
Fig. 3 Fuel cell cascade system



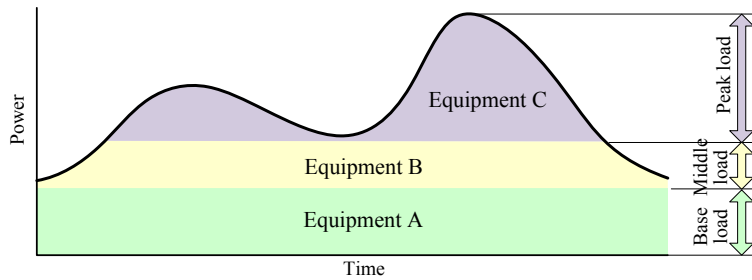
(a) Single piece of equipment



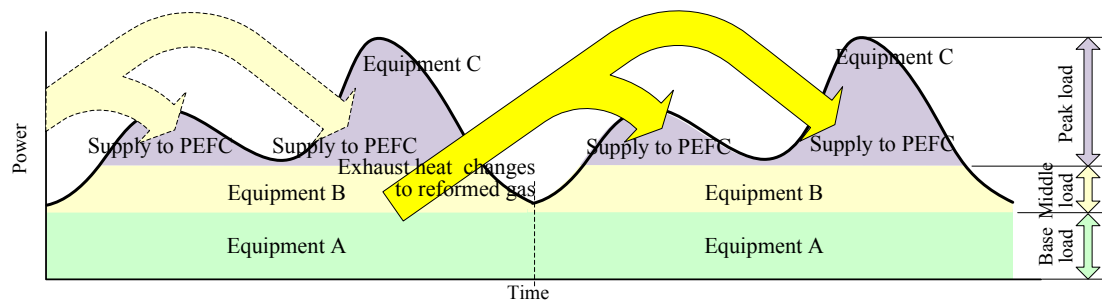
(b) Two types of equipment in a combined cascade system



(c) Two types of equipment in a combined cascade system with time shift utilization of reformed gas

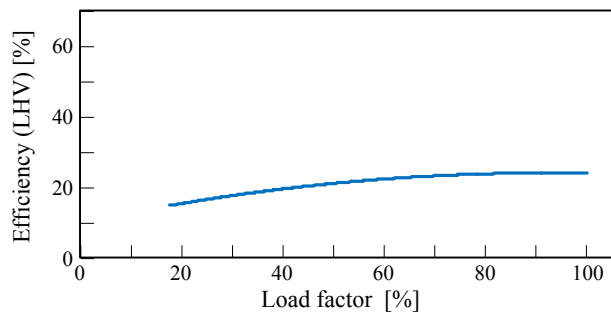


(d) Three types of equipment in a combined cascade system

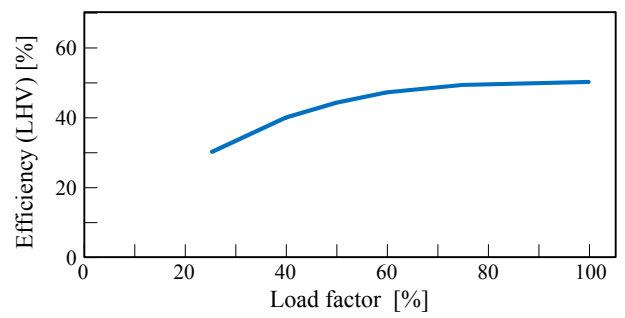


(e) Three types of equipment in a combined cascade system with time shift utilization of reformed gas

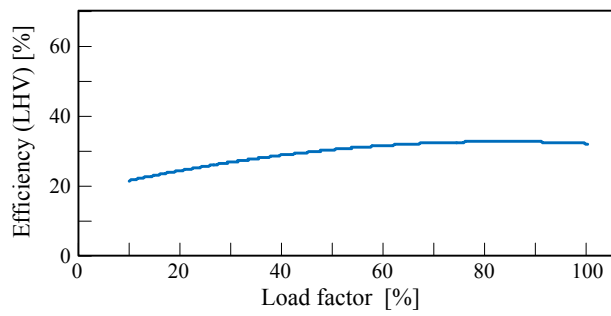
Fig. 4 Operation methods of fuel cell cascades incorporated into a microgrid



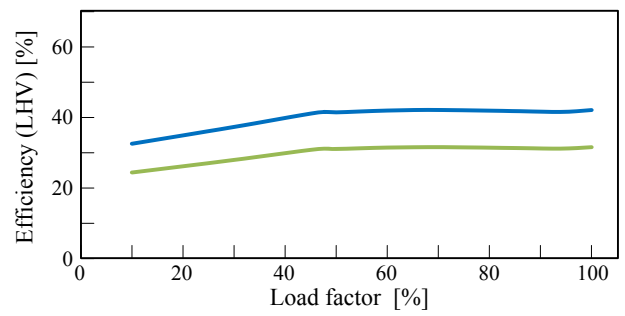
(a) Micro-gas turbine (MGT)



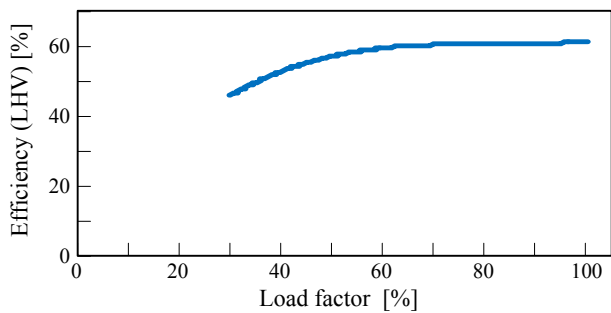
(b) SOFC



(c) Natural-gas-supplied PEFC



(d) Methanol reformed gas-supplied PEFC



(e) SOFC and MGT combined system

— Without reformer efficiency
 — With reformer efficiency

Fig. 5 The relationship between the load factor and the power generation efficiency for each piece of equipment

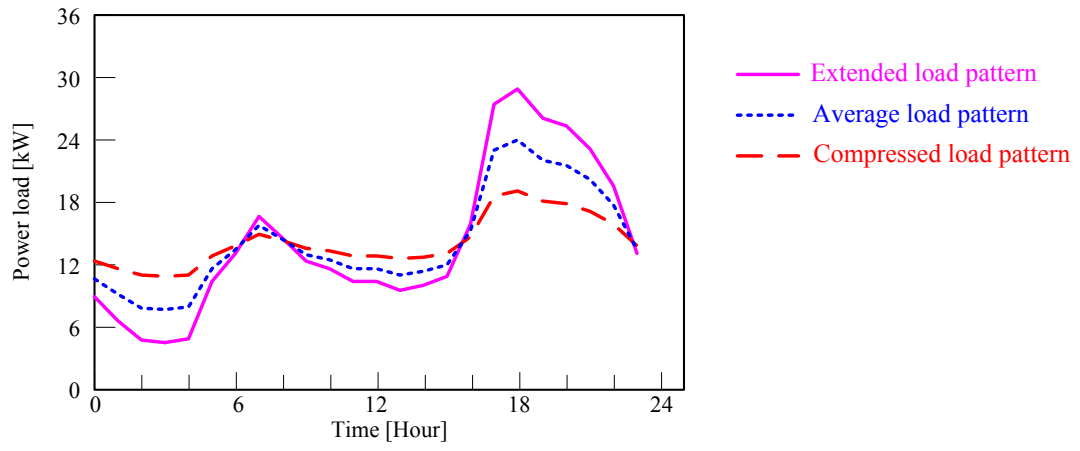
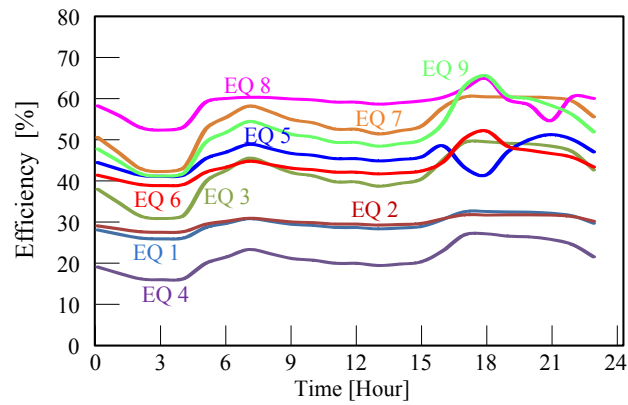
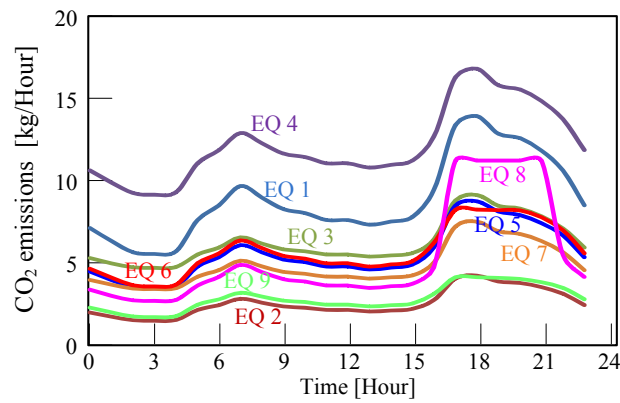


Fig. 6 Power demand pattern of the microgrid (Sapporo Japan, 30 houses, February representative day)

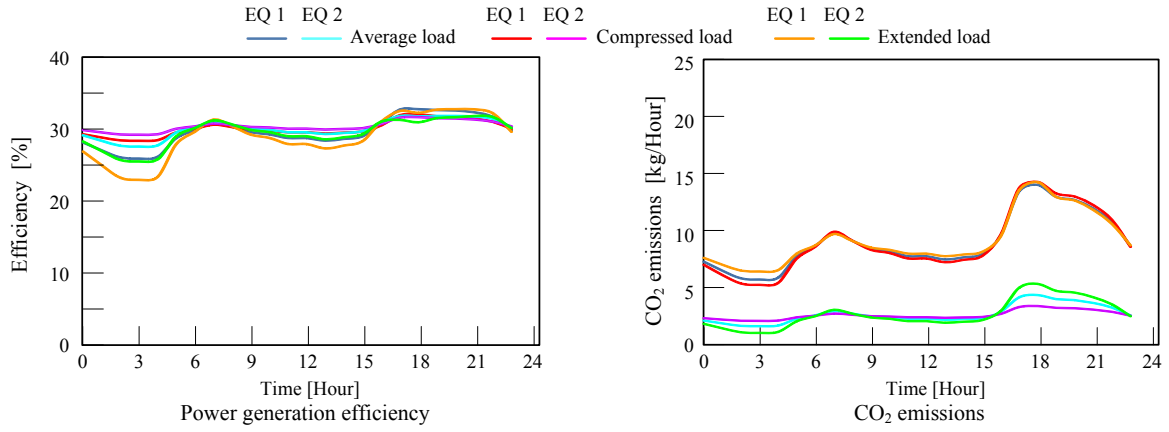


(a) Average power generation efficiency

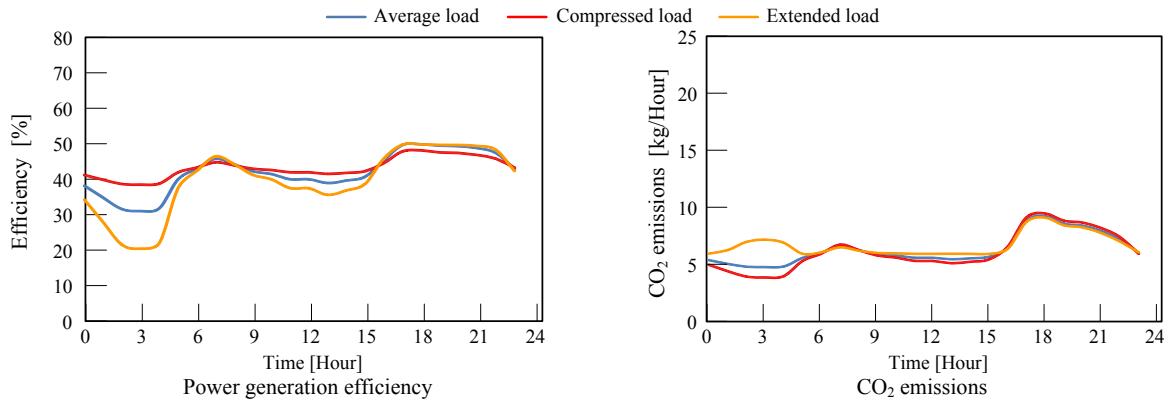


(b) CO₂ emissions

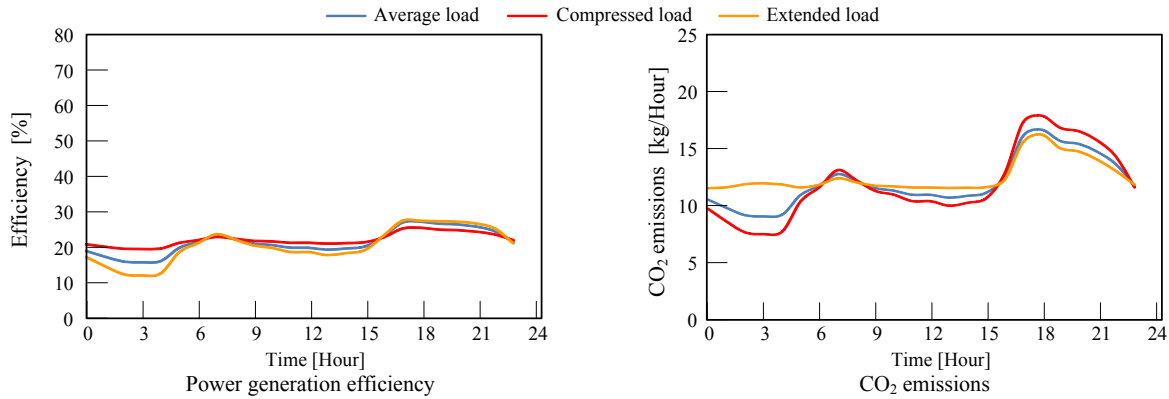
Fig. 7 Analysis results for the power generation efficiency and the CO₂ emissions for each piece of equipment under the average load pattern



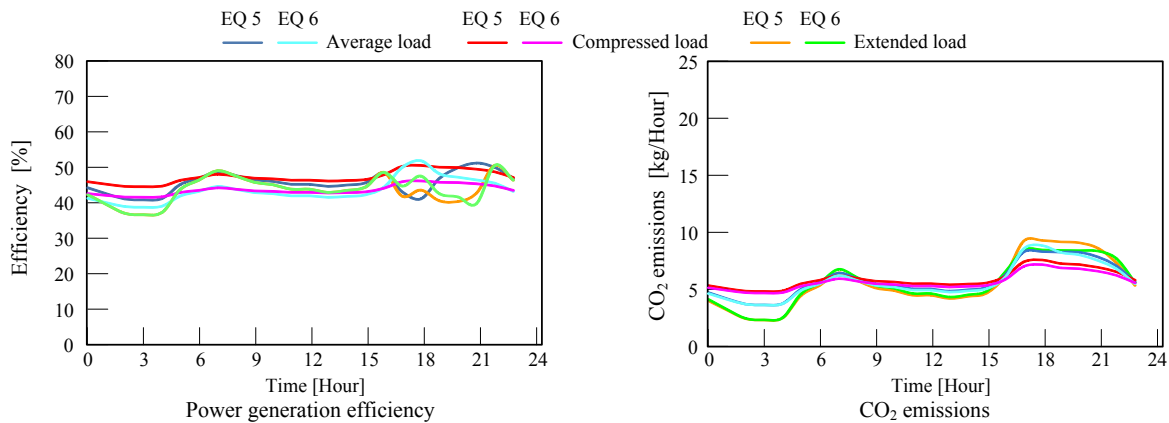
(a) PEFC (EQ 1, EQ 2)



(b) SOFC (EQ 3)



(c) MGT (EQ 4)



(d) SOFC-PEFC combined system (EQ 5, EQ 6)

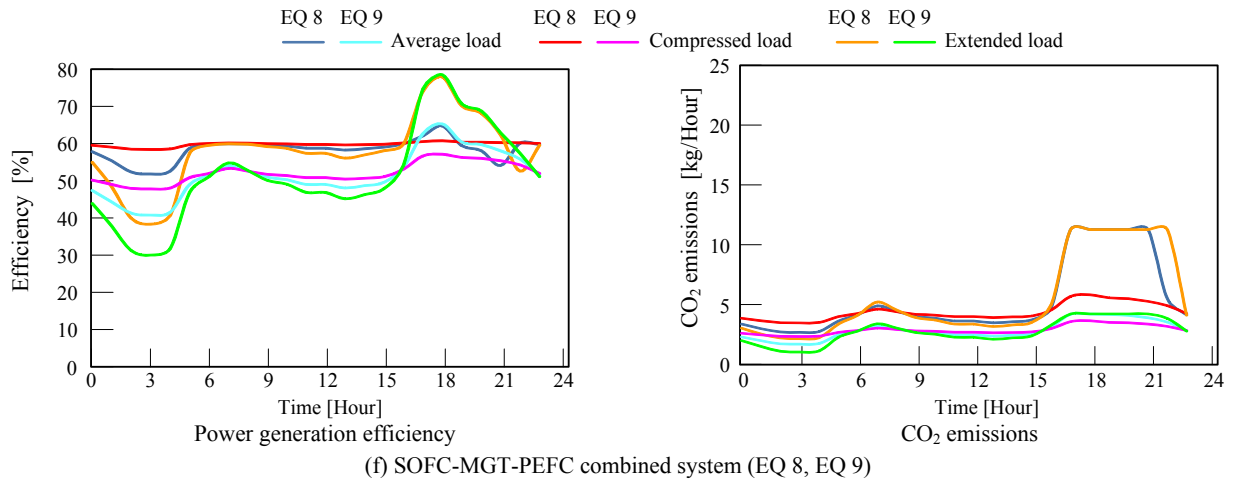
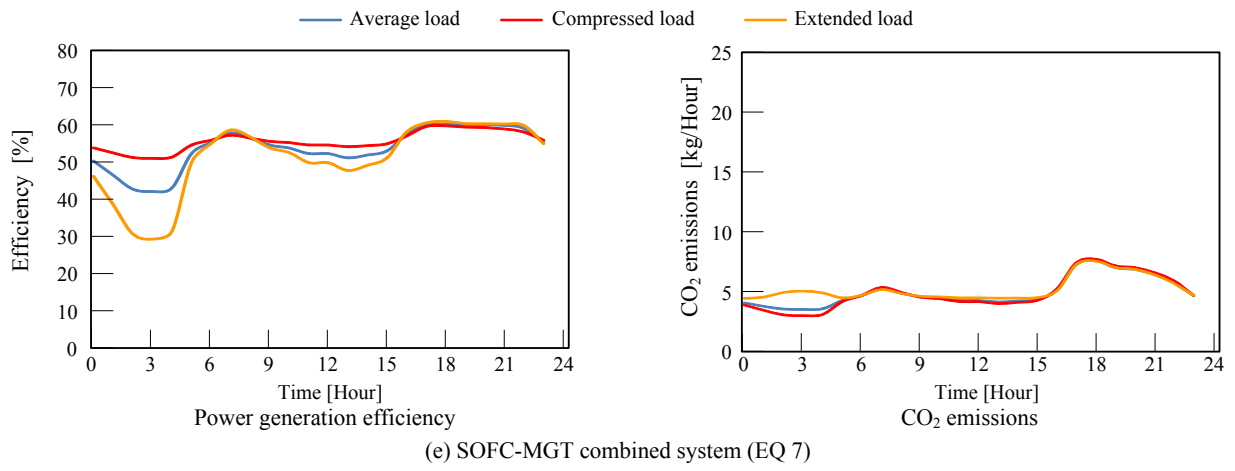
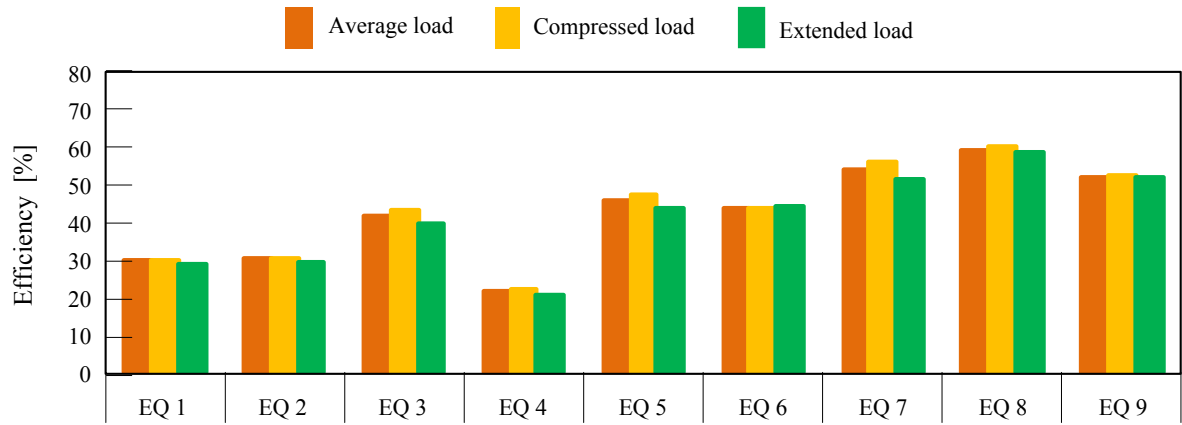
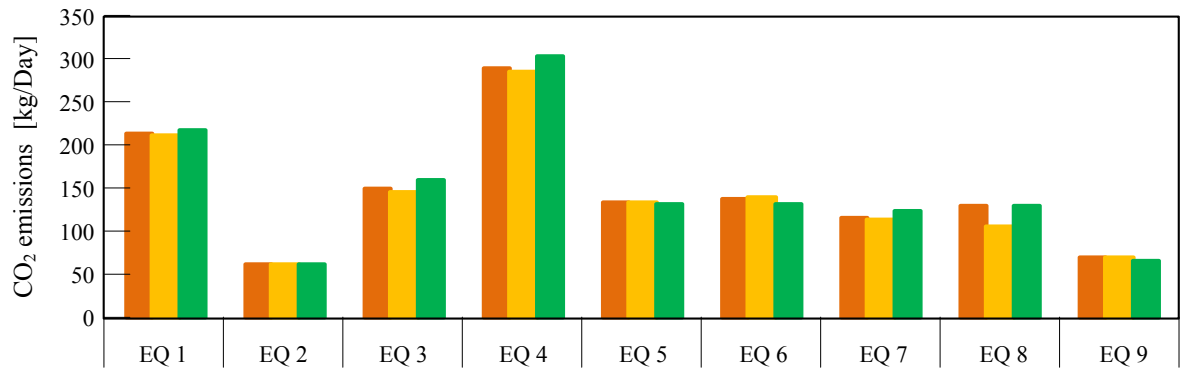


Fig. 8 Analysis results for the power generation efficiency and the CO₂ emissions of each piece of equipment under three load patterns



(a) Power generation efficiency



(b) CO₂ emissions

Fig. 9 Analysis results for the daily average power generation efficiency and CO₂ emissions

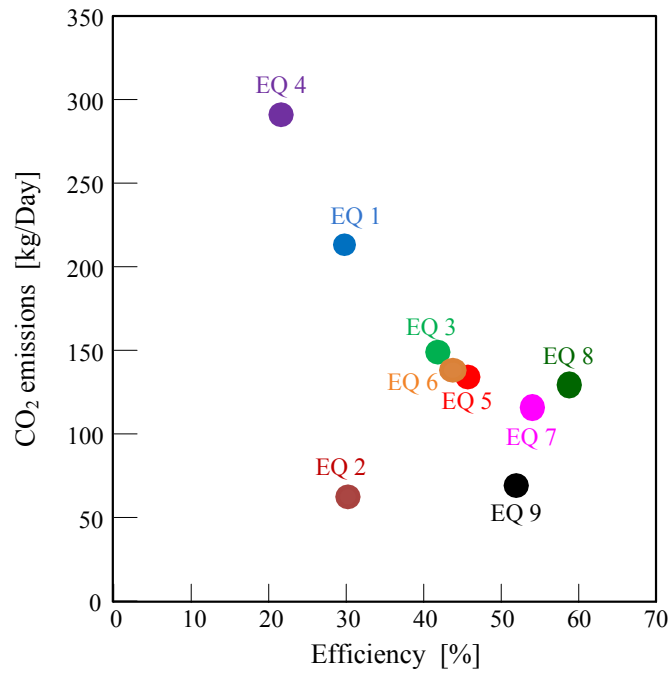


Fig. 10 Analysis results for the daily average power generation efficiency and CO₂ emissions